# CHAPTER 2

# CHAPTER 2

## Combined Phase Behavior, Dynamic Light Scattering, Viscosity and Spectroscopic Investigations on Pyridinium Based Ionic Liquid-in-Oil Microemulsion


### Abstract

Although several studies on imidazolium based ionic liquid-in-oil microemulsion are available in the literature, however, studies on pyridinum bases ionic liquid microemulsion are not so common. Pyridinium based ionic liquids have superior yet unexplored properties when considered in the polar domain of microemulsion. 1-butyl-4-methyl pyridinium tetrafluoroborate ([b4mpy][$BF_4$]) / (Tween 20 + n-pentanol) / n-heptane microemulsion system has been studied by combined phase behavior, dynamic light scattering, viscosity and spectroscopic probing techniques. With the increasing amount of Tween 20/n-pentanol (S/CS) ratio, turbidity increased, although it was not possible to achieve a stable microemulsion without the cosurfactant. Dynamic light scattering and viscosity study revealed that the size of the μE droplets increased with increasing volume fraction ($\varphi_d$) of ionic liquid. Both the size and viscosity increased with $\varphi_d$. With the increasing amount of n-pentanol, the variation became less sensitive due to the better stabilizing effect induced by the alkanol. Increase in size of the microemulsion droplets was overshadowed by the increase in the fluidity of the medium, for which viscosity decreased with increasing temperature, as common for Newtonian fluids. State of the ionic liquid in the microemulsion was monitored by absorption and fluorescence spectroscopy with and without curcumin as the molecular probe. While a continuous increase in polarity of the IL domain occurred with increasing amount of IL, the fluorescence anisotropy results revealed that the rigidity of the domain passed through maxima for all S/CS ratio.



Communicated to RSC Advances, Manuscript ID: RA-ART-02-2014-001209

## 1. Introduction

Because of the multifaceted applications, viz., drug delivery, nanoparticle synthesis, media for organic reaction, biochemical reaction, separation, cosmetics[128], etc., studies on microemulsion (μE) have gained significant importance. A microemulsion (μE) can be defined as an optically transparent, thermodynamically stable dispersion of one liquid in otherwise immiscible second liquid, stabilized by a surfactant[34]. Sometimes, short chain alkanols and amines can assist μE formation[220]. It has been reported that ionic liquid (IL) can substitute the polar component (water) in a μE[225]. Scientific studies involving ILs have reached its credential beyond any doubt for which there has been an exponential growth in the research publication involving ILs. By definition ILs, with melting points below $100^0$C, are considered as neoteric component for its specific properties, viz., non-flammability, non-corrosiveness, high ionic conductivity and inertness towards different thermal and chemical environment[185]. One of the outstanding properties of ILs lies in its use as an alternative to traditional organic solvents. ILs are also called "designer solvents" because its properties can be tuned by altering the substituent as well as the counter ions[235]. In spite of significant research contribution on ILs, the lack of complete knowledge is considered to be one of the barriers in utilizing them for practical applications. Thus more fundamental researches on ILs are warranted.

It is needless to mention that μE comprising ILs in the polar domain can have some unknown but some novel properties owing to the unique and combined features of the ILs and μEs. Thus, this domain of research has been gaining significance day by day. Ionic liquid microemulsions find application in various fields, viz., preparation and characterization of polymeric nanoparticles[236], synthesis of inorganic nanoparticles[237], renewable lubricants[238], and catalysis[239], etc.

Although most of the studies on ILs are associated with the imidazolium ion, however, there has been a current trend to search for alternate, easily available but low cost ILs other than the imidazolium ion. According Domanska et al.[240], pyridinium based ILs have specific properties, viz., broad liquidous

temperature range, inertness to air, moisture and superior solubilization capacity. These unique features of pyridinium based ILs have already been explored with special reference to antistatic thermoplastic resin[241], adhesive film[242], electrochemical probe[243], electron transfer process[244], reaction acceleration[245], organo catalysis[246], extraction process[247], etc. In spite of high possible potentials, there have been a little research on 1-butyl-4-methylpyridinium tetrafluoroborate ([b4mpy][$BF_4$]) comprising μE although it is one of the most reported pyridinium based IL[248]. In a very recent report of Takumi et al.[249], mutual miscibility of imidazolium and pyridinium ILs with $[BF_4]^-$ as the common counter anion have been explored. Another advantage of using this IL is that the system itself can be investigated without any molecular probe (because of the presence of the pyridinium ring) in the UV-visible region.

Curcumin is a natural polyphenolic compound isolated from the rhizome of turmeric (Curcuma longa). Researches over the last few decades have shown that curcumin possesses a great variety of beneficial biological and pharmacological activities such as anticancer, antioxidant, anti-arthritic, and anti-inflammatory agents[250]. Despite its highly promising features as a health-promoting agent, poor aqueous solubility in neutral aqueous medium of curcumin[251] is one of the major draw backs in its bioavailability, clinical efficiency and metabolism[252]. A number of attempts have been made to increase the solubility in polar medium and hence the bioavailability of curcumin through encapsulation in surfactant micelles[253,254], lipids[255], cyclodextrin[256], hydrogel[257], liposomes[258], polymeric micelles[259], nanoparticles[260], etc. Curcumin is also soluble in other polar solvents, so there is a huge scope of its bioavailability if it can be entrapped in μE with a polar phase. Once used in the IL-in-oil microemulsion, curcumin may have a possibility to reside in the inner polar core of the μE because curcumin is not soluble in n-heptane. Thus the spectroscopic investigation involving curcumin in the microemulsion will be able to probe the microenvironment of the polar domain

In the present manuscript, comprehensive studies on the IL-in-oil type microemulsion comprising 1-butyl-4-methylpyridinium tetrafluoroborate have been reported. It is expected that studies on such type of μE comprising

[b4mpy][$BF_4$], Tween 20 (a nonionic surfactant, S), n-pentanol (a cosurfactant, CS) and n-heptane (oil) will generate significant information in terms of its practical application as well as the view point of fundamental understanding. The effect of Tween 20(surfactant)/n-pentanol (cosurfactant) ratio, volume fraction of IL and temperature have been studied using a number of techniques, viz., phase manifestation, dynamic light scattering, viscosity, UV-visible absorption and emission spectroscopy. The detailed phase diagram studies helped in identifying the clear and turbid region. Dynamic light scattering studies provided the information about the size and its distribution at different temperature; viscosity measurements were carried out and correlated with the DLS data. μE with and without curcumin in the polar domain were investigated by UV-visible absorption spectroscopy. Fluorescence spectroscopic studies on curcumin in the polar domain helped in understanding the state of polarity and rigidity of the microenvironment.

## 2. Experimental section

**2.1. Materials.** The IL 1-butyl-4-methyl pyridinium tetrafluoroborate, [b4mpy][$BF_4$] was purchased from Sigma-Aldrich Chemicals Pvt. Ltd., USA. The nonionic surfactant polyoxyethylene sorbitan monolaurate (Tween 20) and the cosurfactant n-pentanol were products from Fluka, Switzerland and Lancaster, England respectively. They were stated to be more than 99.5% pure. n-heptane was obtained from E. Merck, Germany. Curcumin, [1,7-bis(4-hydroxy-3-methoxy-phenyl)-1,6-heptadiene-3,5-dione] was a product from Sigma-Aldrich Chemicals Pvt. Ltd., USA. All the chemicals were used as received.

### 2.2. Methods

**2.2.1. Phase manifestation.** In the entire work, three different ratio of Tween 20 and n-pentanol (S:CS, w/w) were used (1:0.5, 1:1 and 1:2) to explore the effect the different amount of cosurfactant in the μE system. The pseudo ternary phase diagram comprising [b4mim][$BF_4$]/(Tween-20+n-pentanol)/n-heptane was constructed by the method of titration and through visual inspection. Known amount of Tween 20 + n-pentanol and n-heptane or IL were taken in stoppered test tube. IL or n-heptane was then progressively added using a

Hamilton (USA) micro syringe under constant stirring[261,262]. The whole process was carried out in a controlled temperature bath (298±0.1K). The phase boundary was detected through the appearance of turbidity. The same experiment was carried out for a number of compositions by varying the amount of oil or IL as well as in different S/CS ratio.

**2.2.2. Dynamic light scattering (DLS) studies.** DLS measurements were carried out using a Zetasizer Nano ZS90 (ZEN3690, Malvern Instruments Ltd, U.K.). A 0.2M Tween 20 mixed with n-pentanol in n-heptane was used for such studies. Tween 20 / n-pentanol ratio (w/w) were the same as in phase manifestation studies. A He-Ne laser of 632.8 nm wavelength was used and the data were collected at $90^0$ angle. Temperature was controlled by inbuilt Peltier heating-cooling device with an accuracy of ±0.05K. The instrument actually measures the diffusion coefficient (D) from which the diameter of the microemulsion droplet (d) was determined according to Stokes-Einstein's formalism[261,262]:

$$D = \frac{kT}{3\pi\eta d} \qquad \textbf{(2.1)}$$

where, k, T and η indicate the Boltzmann constant, temperature and viscosity respectively.

**2.2.3. Viscosity measurement.** Viscosity of μE systems were measured with an LVDV-II+PCP cone and plate type roto-viscometer (Brookfield Eng. Lab, USA). The same set of solution, as used in the DLS measurements, were employed for size analyses. Temperature was controlled by a cryogenic circulatory water bath with a precision of ±0.1K (DC-1006 M/S. Hahntech Corporation, S. Korea). Shear rate (D) was varied in the range 20 – 60 $sec^{-1}$ with an increment of 5.0 $sec^{-1}$ in each step. Zero shear viscosity (η) was obtained using the relation $\eta = \tau / D$ [261,262], where τ indicates the shear stress.

### 2.2.4. Spectral studies.

**Absorption spectra.** UV-visible absorption spectra of the μE systems in the absence and presence of curcumin were recorded on a UVD-2950 spectrophotometer (Labomed Inc., USA) in the range 200-400nm using a matched pair cell of 1.0cm path length. While recording the spectra of the IL comprising systems, corresponding surfactant solution without IL was used as reference. Corresponding IL-in-oil μE without the dye curcumin was used as reference for recording the spectra of curcumin comprising systems. The overall concentration of curcumin was always kept constant at 10 μM. Initially, required amount of curcumin in methanol-chloroform (1:3 v/v) was taken in a test tube. The solvent was evaporated under vacuum. μE of known composition was then added and homogenized by keeping the solution in an ultrasonic water bath. It is to be mentioned that curcumin is insoluble in n-heptane. Therefore it could be assumed that the dye molecules reside in the polar domain.

**Emission spectra.** Steady state fluorescence spectroscopic measurements were carried out using a bench-top spectrofluorimeter (Quantamaster-40, Photon Technology International Inc, NJ, USA). The steady state emission spectra was recorded in the range 400-650nm with an excitation of curcumin at 426nm.

To know about the microviscosity of the solvent surrounding the probe molecule, steady state anisotropy (r) values were determined using the following expressions[263]:

$$r = (I_{VV} - GI_{VH}) / (I_{VV} + 2GI_{VH}) \quad \textbf{(2.2)}$$

and,

$$G = I_{HV}/I_{HH} \quad \textbf{(2.3)}$$

where, $I_{VV}$, $I_{VH}$ are the intensities obtained with the excitation polarizer oriented vertically and the emission polarizer oriented vertically and horizontally respectively; $I_{HV}$ and $I_{HH}$ refer to the similar parameters as above for the horizontal positions of the excitation polarizer. In case of anisotropy measurements, the fluorescence data were collected at an emission wavelength ($\lambda_{em}$) of 550 nm. Further details are available in literature[263]. Both the absorption and fluorescence spectra were recorded at ambient but controlled temperature.

## 3. Results and discuccions

**3.1. Phase manifestation.** From the application point of view, construction of the phase diagram is a primary task towards a μE formulation. Figure 2.1 describes the pseudo ternary phase diagram of [b4mpy][$BF_4$]/(Tween-20+n-pentanol)/n-heptane systems at different surfactant-cosurfactant ratio (w/w).

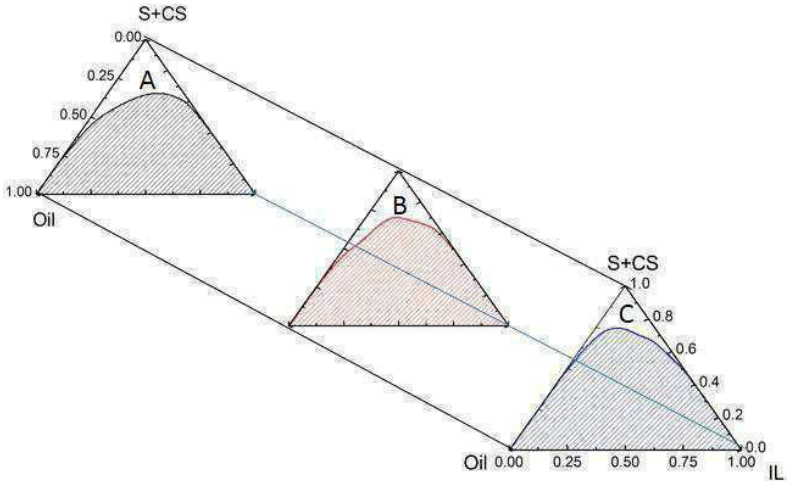


**Figure 2.1.** Pseudo ternary phase diagram of [b4mpy][$BF_4$]/(Tween-20+n-pentanol)/n-heptane at different Tween 20 (S) / n-pentanol (CS) ratio (w/w): A, 1:0.5; B, 1:1 and C, 1:2. n-heptane was used as oil (Oil) and [b4mpy][$BF_4$] was used as the ionic liquid (IL). Temp. 298 K.

For simplicity, only the clear single phase (1Φ, un-shaded portion) and the two phase (2 Φ, shaded portions) regions were identified. Area under the clear and turbid regions were evaluated by the method of weighing the individual areas as previously described[261]. The area under clear zone decreased with increasing amount of cosurfactant. It appeared from the results (as explained through Figure 2,) that the area under the clear zone was maximum in the absence of cosurfactant as the % area of clear zone followed a $2^0$ polynomial relation with the weight% of n-pentanol ($w_{cs}$):

$$\% \text{ area of clear zone} = 20.34 - 8.46 \times w_{CS}\ \% + 1.61 \times (w_{CS}\ \%)^2 \qquad \textbf{(2.4)}$$

It means that in the absence of n-pentanol, % area under clear and turbid zones would be 20% and 80% respectively. However, it was impossible to obtain a stable μE without the aid of cosurfactant. Hence, unlike the other systems[211,225], use of cosurfactant was mandatory in order to achieve a stable μE. Use of cosurfactant for single tailed surfactants is not uncommon in literature[261,262]. It is known that cosurfactant can assist the surfactant molecules in a reducing

interfacial tension between two immiscible liquids. Present set of results were also comparable with the similar components where water[261] and another ionic liquid 1-butyl-3-methyl imidazolium methanesulphonate [bmim][MS][262] were used. Compared to the other systems, the %area under clear zone was less which could be due to the greater iconicity of the components in the polar domain, compared to water as well as [bmim][MS]. Although the cation $[b4mpy]^+$ was less polar, however, the $BF_4^-$ ion played a significant role in enhancing the turbidity of the present μE.

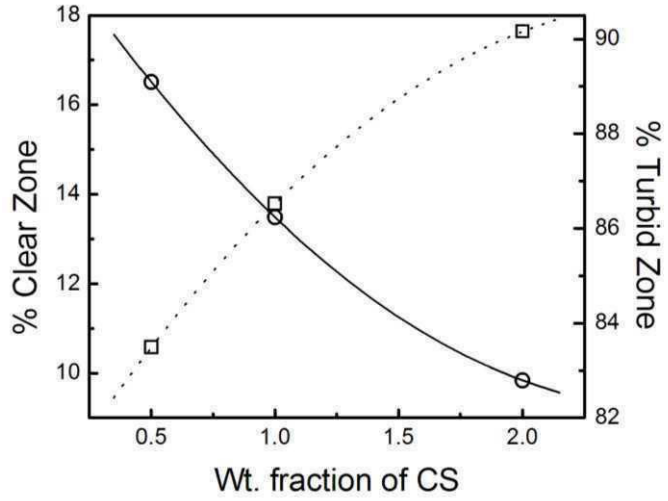


**Figure 2.2.** *Variation in the area under clear (O) and turbid (□) regions with the weight* fraction of n-pentanol (CS) for [b4mpy][$BF_4$]/(Tween-20+ n-pentanol)/n-heptane pseudo-ternary system at 298 K.

**3.2. Dynamic light scattering (DLS) and viscosity studies.** DLS studies on μE can provide information on its size, its distribution, and hence the polydispersity index. Variation in the diameter of [b4mpy][$BF_4$]/(Tween 20+n-pentanol)/n-heptane IL-in-oil μE with the volume fraction of the IL ($\varphi_d$) at 308 K have been graphically presented in Figure 2.3 at different surfactant cosurfactant ratio (panel A).

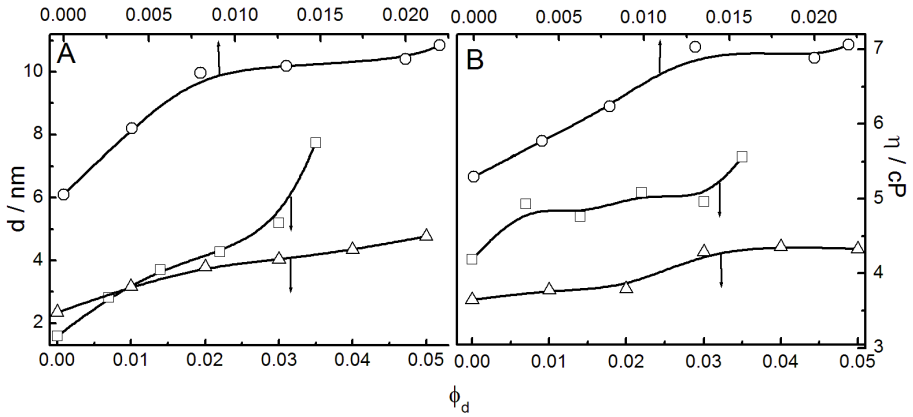


**Figure 2.3.** Variation in d*iameter (d) and viscosity (η) of [b4mpy][BF$_4$]*/(Tween-20+ n-pentanol)/n-heptane IL-in-*oil microemulsion system with the volume fraction (*$\varphi_d$) of [b4mpy][BF$_4$]. Temp. 308 K. Tween 20/ n-*pentanol ratio (w/w): O, 1:0.5; □, 1:1 and* Δ, 1:2.

Droplets were fairly monodispersed as revealed through its size distribution shown in Figure 2.4.

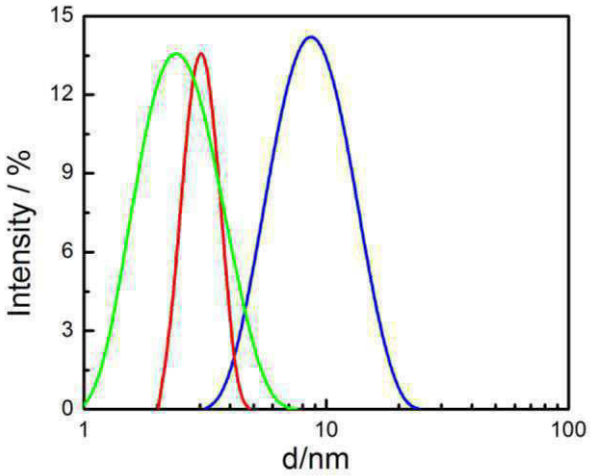


**Figure 2.4.** Dependence of size distribution on Tween20/n-pentanol (S/CS) ratio for [b4mpy][BF$_4$]/(Tween-20+n-pentanol)/n-heptane IL-in-oil microemulsion systems. Tween 20/ n-pentanol ratio (w/w): 1:0.5, blue line; 1:1, red line and 1:2, green line.

As under similar condition, there is a correlation between the size of droplets and viscosity, hence the viscosity (η) – $\varphi_d$ profile for the similar systems were also presented in the same Figure (panel B). Experiments were carried out in the temperature range 293 – 323K and the results at 308K (intermediate temperature) have been shown as representative. Results for the other systems have been presented in the supplementary section. Size of the μE droplets increased with increasing volume fraction ($\varphi_d$) of IL. Increase in size with the

increasing volume of the dispersed phase is not an uncommon phenomena and have also been observed by others[113,176,211,225,262]. Size - $\varphi_d$ profiles were found to be dependent on the S/CS ratio. Size of the μE droplet comprising Tween 20 and n-pentanol in a mass ratio of 1:0.5 was found to be larger than 1:1 which was even larger than 1:2. Results clearly indicate that cosurfactants caused size constriction. In a previous report we have shown that for the polyoxyethylene head group comprising surfactants (Tween 20), increased amount of cosurfactant can lead to the formation of larger number of droplets[261,262]. For a fixed amount of surfactants, increasing number of droplets would result only if the size is decreased. Such an observation further supports the decrease in the area under clear region with increasing amount of cosurfactant. While giving a closer look at the panel A of Figure 3 it was observed that for an S / CS ratio of 1:0.5, size of the μE droplet increased linearly up to $\varphi_d$=0. 01, after which a change in the slope of increment profile appeared. The results imply that the existence of free/unbound ILs was possible only after $\varphi_d$=0. 01. Before the said volume fraction of IL, it is mainly used up in coordinating with the polyoxyethylene head groups of Tween 20[262]. Almost twice the volume of IL was required for the attainment in the breakpoint in the μE with S/CS ratio 1:1 ($\varphi_d$=0.02). However, for such systems the slope after the threshold was higher. Such an ambiguity is beyond explanation with the present level of knowledge. Further studies are warranted to address this issue. d vs. $\varphi_d$ profile for the systems with surfactant/cosurfactant ratio 1:2 was almost linear. d-$\varphi_d$ profile for all the systems at different temperature have been graphically presented in Figure 2.5. It could be concluded from the results that with the increasing amount of cosurfactant (n-pentanol), size increment with the volume fraction becomes less sensitive. The viscosity profile for the similar systems followed the same trend line as in the variation of droplet size with $\varphi_d$. Thus, it could be concluded that variations in the viscosity with $\varphi_d$ was a consequence of the size variation in the microemulsion droplets. In order to understand the effect of temperature, size measurements were also carried out at different temperatures (293, 298, 303, 308, 313, 318 and 323K).

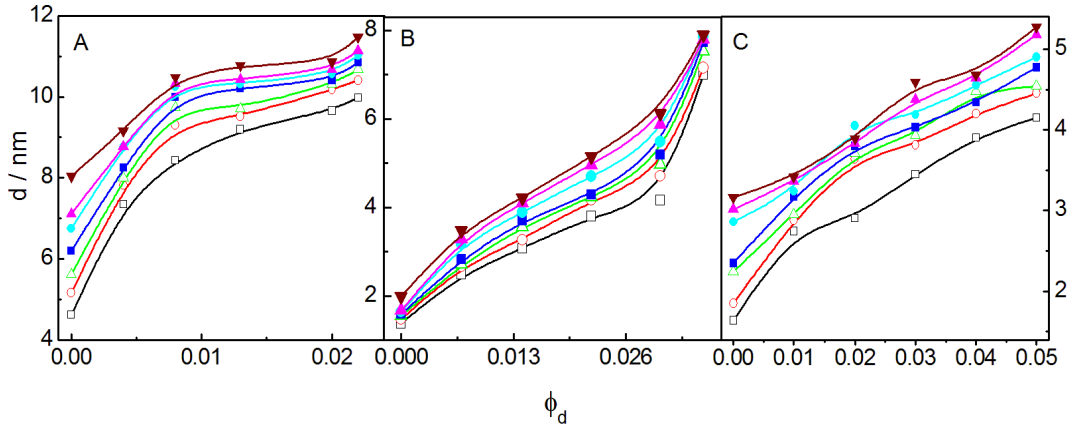


**Figure 2.5.** Variation in size (d) of [b4mpy][$BF_4$]/(Tween-20+n-pentanol)/n-heptane IL-in-*oil microemulsion systems with the volume fraction* ($\varphi_d$) of IL. Tween 20/n-pentanol *ratio (w/w): A, 1:0.5; B, 1:1 and C, 1:2. Temp. (K):* □, *293;* O, *298;* Δ, *303;* ■, *308;* ●, *313;* ▲, *318 and* ▼, *323.*

While considering the size variation (as shown in Figure 2.6 panel A), it was observed that for all the systems d vs. temperature profiles were almost linear. The parallel nature of the lines imply that the effect of temperature was independent of S/CS ratio. Although there occurred size increment with increasing temperature, however, reverse trends were recorded for the viscosity for all the systems. Results for viscosity-temperature profile for the three combinations at $\varphi_d$= 0.02 have been shown in Figure 2.6 (panel B).

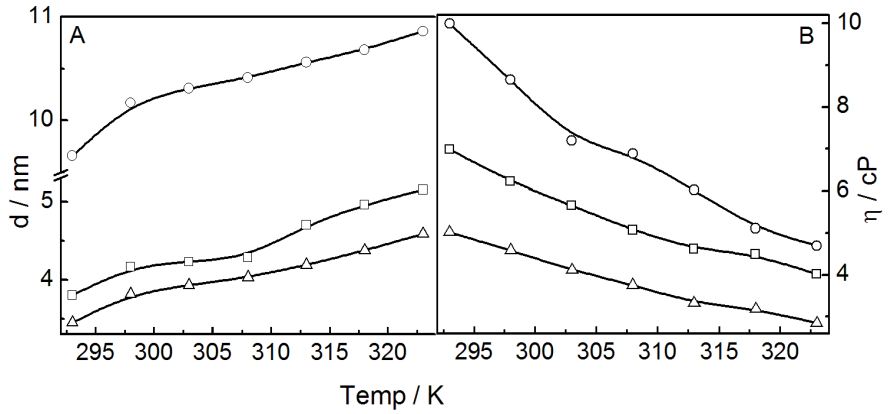


**Figure 2.6.** Variation in the size (A) and viscosity (B) with temperature for [b4mpy][$BF_4$]/(Tween-20+n-pentanol)/n-heptane IL-in-oil microemulsion at different Tween 20/n-pentanol ratio *(S/CS, w/w): O, 1:0.5;* □, *1:1 and* Δ, *1:2. 0.2 M Tween20 was used in each case where the volume fraction* ($\varphi_d$) of IL was kept constant at 0.02.

Decrease in viscosity with increase in temperature is a common phenomenon for Newtonian fluids. In the present set of studies, increase in droplet size was overshadowed by the increase in the fluidity of the medium. For

all the three systems, viscosity decreased almost linearly with increasing temperature, although the slopes were different for the different systems. Differences in the slopes were due to the differences in the rigidity of the μE droplets. Systems with larger amount of cosurfactant are expected to form more rigid structures. By suitably analyzing the viscosity data, thermodynamic parameters, viz., changes in specific heat capacity (ΔCp), activation enthalpy (ΔH*), free energy (ΔG*) and entropy (ΔS*) were evaluated. The activation enthalpy for the viscous flow and the associated entropy change could be expressed by the following equations [127]:

$$\eta = (\frac{hN}{V}) e^{\Delta H^*/RT} e^{-\Delta S^*/RT} \quad \textbf{(2.5)}$$

The logarithmic form of equation 1 could be expressed as:

$$\ln\eta = \left\{\ln\left(\frac{hN}{V}\right) - \frac{\Delta S^*}{R}\right\} + \frac{\Delta H^*}{RT} \quad \textbf{(2.6)}$$

h, N, V are Plank's constant, Avogadro's constant and molar volume respectively. R and T have their usual significances. From equation (2.2), one can obtain $\Delta H^*$ values from the slope of ln η vs $T^{-1}$ plot. ln η was found to vary with $T^{-1}$ in a binomial way; hence one can derive $\Delta H^*$ from it's differential with respect to temperature in the following way:

$$\ln\eta = a + bT + cT^2 \quad \textbf{(2.7)}$$

Therefore,

$$\frac{d\ln\eta}{dT} = -\frac{\Delta H^*}{RT^2} = b + 2cT \quad \textbf{(2.8)}$$

Thus, knowing the value of 'b' and 'c' one can compute $\Delta H^*$ at different temperatures.

Change in heat capacity ($\Delta C_p$) is related to $\Delta H^*$ as:

$$\Delta C_p = \frac{d(\Delta H^*)}{dT} = -2RT(b + 3cT) \quad \textbf{(2.9)}$$

Therefore, changes in Gibb's free energy for activation could be expressed as:

$$\Delta G^* = -RT \ln\frac{\eta V}{hN} \quad \textbf{(2.10)}$$

Once $\Delta H^*$ and $\Delta G^*$ are known, the $\Delta S^*$ value could be calculated easily according to the following expression:

$$\Delta S^* = \frac{\Delta H^* - \Delta G^*}{T} \qquad \textbf{(2.11)}$$

Some of the representative results are summarized in Table 2.1. While considering the changes in the standard enthalpy ($\Delta H^*$), it was observed that for all the systems $\Delta H^*$decreased with increase in the volume fraction ($\varphi_d$) of the dispersed phase. For the systems comprising surfactant and cosurfactant in a ratio of 1:0.5 and 1:1 (w/w), the $\Delta H^*$values were mostly negative, which mean that the process of flow was exothermic in nature [114,127]. On the other hand $\Delta H^*$ for the system with surfactant cosurfactant ratio 1:2 (w/w) the values were mostly positive, the difference in rigidity and subsequent viscosity attributed to such variation. While considering the variation in the $\Delta C_p$ with volume fraction, it was observed that the $\Delta C_p$ attained more negativity with increase in volume fraction. As with the increase in size droplets become less rigid, hence $\Delta C_p$ becomes more negative. The negative value of $\Delta S^*$ indicates the non-spontaneity of the flow processes.

Viscosity variation for all the systems at different volume fractions and temperature have also been graphically presented in Figure 2.7.

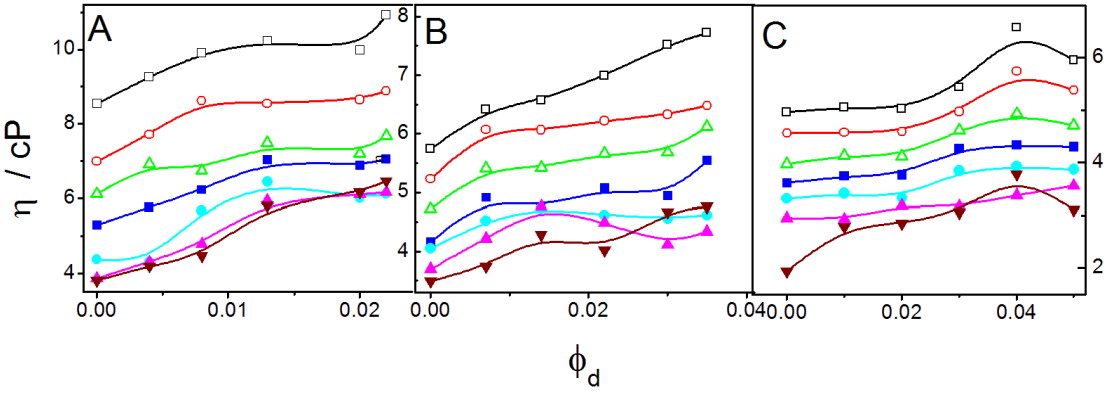


**Figure 2.7.** *Variation in viscosity (η) of [b4mpy][BF$_4$]*/(Tween-20+n-pentanol)/n-heptane IL-in-oil microemulsion *with the volume fraction ($\varphi_d$)* of IL. Tween 20/n-pentanol *ratio (w/w): A, 1:0.5; B, 1:1 and C, 1:2. Temp. (K): □, 293; O, 298; Δ, 303; ■, 308; ●, 313; ▲, 318 and ▼, 323.*

**Table 2.1.** Representative viscosity derived energetic parameters for [b4mpy][$BF_4$]/(Tween-20+n-pentanol)/n-heptane IL-in-oil microemulsion system.

| **Tween 20 / n-pentanol** | **$\varphi_d$** | **$\Delta H^*$( kJ $mol^{-1}$)/$\Delta C_P$(kJ $mol^{-1}$) / -$\Delta G^*$(kJ $mol^{-1}$)/ $\Delta S^*$(J $k^{-1}mol^{-1}$) at different temperature ( in K)** | | | | | | |
|---|---|---|---|---|---|---|---|---|
| | | **293** | **298** | **303** | **308** | **313** | **318** | **323** |
| **1:0.5** | **0.000** | -1.18/-0.95/-0.14/-3.55 | -1.24/-0.99/-0.15/-4.27 | -1.02/-0.17/-1.3/-1.54 | -1.36/1.05/-0.19/-3.28 | -1.09/-0.19/-1.43/-4.61 | -1.12/-0.20/-1.50/-5.43 | -1.16/-0.25/-1.58/-3.55 |
| | **0.004** | -1.52/-1.20/-0.27/-3.66 | -1.60/-1.25/-0.27/-4.46 | -1.29/-0.27/-1.68/-1.64 | -1.33/-0.27/-1.76/-3.52 | -1.37/-0.27/-1.85/-4.97 | -1.42/-0.27/-1.94/-5.81 | -1.46/-0.28/-2.04/-3.66 |
| | **0.013** | -1.56/-2.67/-0.60/-3.80 | -1.65/-2.76/-0.60/-4.83 | -2.85/-0.61/-1.73/-1.92 | -2.95/-0.62/-1.82/-3.90 | -3.04/-0.62/-1.91/-5.58 | -3.14/-0.63/-2.00/-6.59 | -3.24/-0.64/-2.10/-3.80 |
| | **0.022** | -3.18/-3.25/-1.59/-4.09 | -3.34/-3.37/-1.61/-5.25 | -3.48/-1.64/-3.51/-2.17 | -3.60/-1.66/-3.69/-4.31 | -3.71/-1.68/-3.87/-6.26 | -3.83/-1.71/-4.06/-7.39 | -3.95/-1.74/-4.26/-4.09 |
| **1:1** | **0.000** | -0.57/-0.50/-0.03/-1.84 | -0.52/-0.06/-0.60/-1.81 | -0.54/-0.08/-0.63/-1.83 | -0.56/-0.08/-0.66/-1.88 | -0.57/-0.09/-0.69/-1.91 | -0.59/-0.09/-0.72/-1.97 | -0.61/-0.11/-0.76/-2.01 |
| | **0.007** | 0.32/-0.58/-0.06/-1.30 | -0.60/-0.07/0.34/-1.38 | -0.62/-0.08/0.36/-1.47 | -0.64/-0.09/0.38/-1.54 | -0.66/-0.11/0.40/-1.63 | -0.68/-0.14/0.41/-1.73 | -0.71/-0.15/-0.43/-1.80 |
| | **0.014** | -1.14/-0.80/-0.18/-3.28 | -0.82/-0.21/-1.20/-3.32 | -0.87/-0.23/-1.26/-3.40 | -0.90/-0.26/-1.33/-3.47 | -0.93/-0.31/-1.39/-3.45 | -0.97/-0.33/-1.46/-3.55 | -1.14/-0.36/-1.53/-3.62 |
| | **0.030** | -2.65/-2.71/-0.59/-7.04 | -2.80/-0.59/-2.78/-7.32 | -2.90/-0.61/-2.93/-7.65 | -2.99/-0.62/-3.07/-7.94 | -3.09/-0.64/-3.23/-8.29 | -3.19/-0.65/-3.38/-8.59 | -3.29/-0.66/-3.55/-8.94 |
| **1:2** | **0.000** | -0.12/-0.39/0.12/1.74 | -0.12/-0.40/0.12/1.74 | -0.13/-0.41/0.13/1.78 | -0.13/-0.41/0.14/1.79 | -0.14/-0.42/0.14/1.79 | -0.14/-0.43/-0.15/1.82 | -0.14/-0.44/0.16/1.86 |
| | **0.010** | -0.17/-0.40/0.26/2.25 | -0.17/-0.41/0.28/2.32 | -0.18/-0.42//0.29/2.34 | -0.18/-0.43/0.31/2.40 | -0.19/-0.44/0.32/2.43 | -0.19/-0.46/0.34/2.52 | -0.20/-0.46/0.36/2.54 |
| | **0.030** | -0.32/-0.52/-0.93/-1.40 | -0.34/-0.53/-0.98/-1.51 | -0.35/-0.54/-1.03/-1.62 | -0.38/-0.55/-1.08/-1.72 | -0.39/-0.56/-1.13/-1.82 | -0.42/-0.57/-1.18/-1.92 | -0.43/-0.59/-0.24/-2.01 |
| | **0.050** | -0.95/-0.63/0.16/2.70 | -0.98/-0.71/0.17/2.95 | -1.02/-0.79/0.18/3.20 | -1.05/-0.81/0.19/3.25 | -1.08/-0.83/0.20/3.29 | -1.12/-0.88/0.21/3.43 | -1.16/-0.91/0.22/3.50 |

**3.3. Spectral studies.** Spectroscopic investigation on μE using a suitable probe can provide information on the environment, viz., polarity, fluidity, extent of aggregation of the ionic liquid in μE. Substantial reports on such aspects are available in the literature[113,176,225,262]. For the present system as the ionic liquid itself exhibits UV-visible absorption band due to the presence of pyridinium ring, the μE was studied without any probe. Figure 2.8 describes the absorption spectra of [b4mpy][$BF_4$] confined in the polar domain at different volume fraction. Two distinct peaks, one at 280nm and another at 335 nm were recorded for the ionic liquid. The peak at 280nm was significantly more intense than the other. Intensity of both the bands increased with the increasing volume fraction ($\varphi_d$) of ionic liquid. Absorbance vs. $\varphi_d$ profile for both the peaks have been graphically shown in the inset of Figure 2.8. An increment in the absorbance values were mostly linear except for the system with Tween 20/n-pentanol in a ratio of 1:0.5 (w/w). The results indicate that distinct structured aggregates were not formed at this composition. The combined phase manifestation, dynamic light scattering and viscosity data also supported such an analogy.

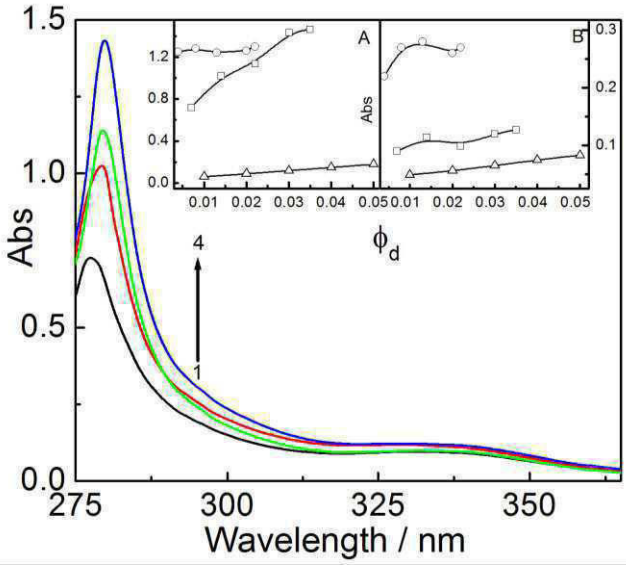


**Figure 2.8.** Absorption spectra of 1-butyl 4-methyl pyridinium tetrafluoroborate [b4mpy][$BF_4$] *confined in the polar domain at different volume fraction* ($\varphi_d$): 1, 0.007; 2, 0.014; 3, 0.022 and 4, 0.03. System without the IL was used as reference. Inset: Variation *in the absorbance at 283 nm (A) and 335 nm (B) with* $\varphi_d$.

Effect of IL was different for different Tween 20/ n-pentanol combinations; hence in order to understand the state of the IL, curcumin was used

as the fluorescent probe. Fluorescence spectra of curcumin confined in the polar domain of ionic liquid-in-oil microemulsion are shown in Figure 2.9. When excited at 426 nm, curcumin shows an emission maximum at ~500 nm. Results were found to be comparable with the previous reports[264]. A red shift in the emission maximum alongwith a decrease in fluorescence intensity with the increase in the $\varphi_d$ value were noted (Inset: panel A, Figure 2.9). This was due to the localized dilution of the probe in the IL pool[113,133,205,262] . The progressive red shift (Inset: panel B, Figure2.9) in the emission maxima was due to the increased polarity of the domain with increasing volume fraction of the ionic liquid[262].

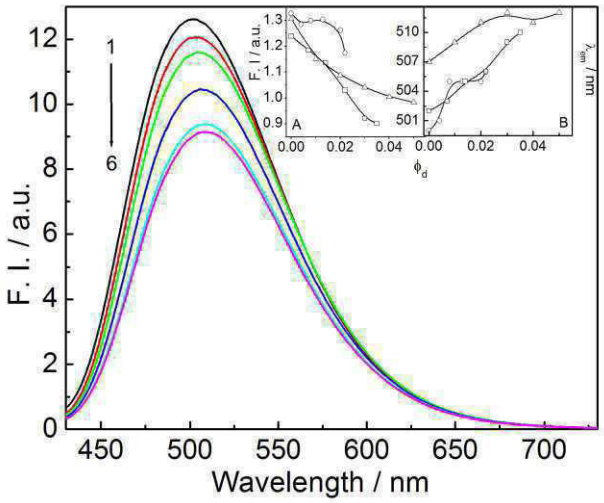


**Figure 2.9.** Emission spectra of 10 µM curcumin in [b4mpy][$BF_4$]/(Tween-20+n-pentanol)/n-heptane IL-in-*oil microemulsion at different volume fraction ($\varphi_d$) of IL.* $\varphi_d$ values: 1, 0.00; 2, 0.007; 3, 0.014; 4, 0.022; 5, 0.03 and 6, 0.035. Tween 20/n-pentanol *ratio (w/w): l:1. Inset: Variation in the fluorescence intensity (panel A) and* $\lambda_{em}$ (panel B) with $\varphi_d$ for different Tween 20/n-*pentanol ratio (w/w): O, l:0.5; □, 1:1 and Δ, 1:2.*

To know the exact state of the solvent in the pool, fluorescence anisotropy studies on curcumin was carried out. Variation of fluorescence anisotropy value (r) with the volume fraction ($\varphi_d$) of ionic liquid have been graphically shown in Figure 2.10.

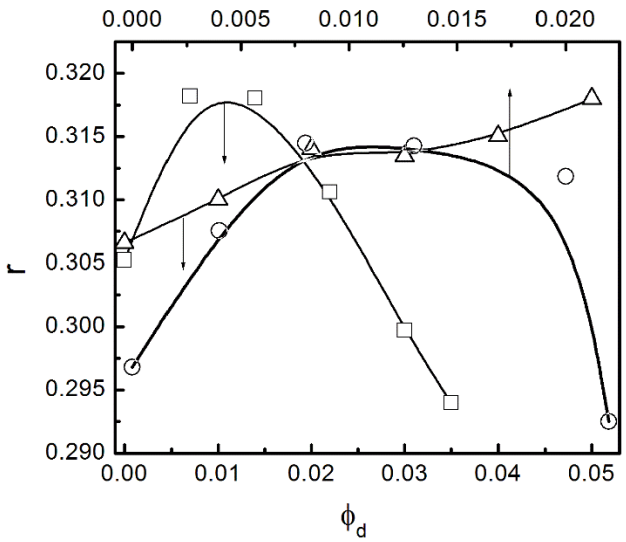


**Figure 2.10.** *Variation in the fluorescence anisotropy (r) for 10 μM curcumin with different volume fraction ($\varphi_d$)* of IL for [b4mpy][$BF_4$]/(Tween-20+ n-pentanol)/n-heptane IL-in-oil microemulsion system. Tween 20/n-*pentanol ratio (w/w): O, 1:0.5; □, 1:1 and* Δ, 1:2. Temp, 298K.

Anisotropy values passed through maxima with respect to the volume fraction of IL. Initially ILs are used up in coordinating with the oxyethylene head groups of Tween 20 for which structured entities are formed. At that stage the dye molecules did not have the freedom of movement. After the process of coordination of surfactant head group by IL cation was over, excess IL became free for which they can behave as bulk IL. Under that situation, the mobility of dye molecules became higher. This eventually led to the decrease in the fluorescence anisotropy values. A linear increase in the anisotropy value for the system comprising Tween20:n-pentanol in a 1:2 w/w ratio was due to the continued solvation of the cationic component of the ionic liquid, which was assisted by the presence of larger number of alkanols.

## 4. Summary and conclusion

Comprehensive studies on 1-butyl-4-methyl pyridinium tetrafluoroborate ([b4mpy][$BF_4$]) / (Tween 20 + n-pentanol) / n-heptane microemulsion system were carried out using a number of different physico-chemical techniques. Although the cosurfactant increased turbidity of the microemulsion, however, it was required for the attainment of stable microemulsion. Cosurfactant controlled

the curvature of the microemulsion droplets; it simultaneously also imparted better stability by solvating the cationic component of the ionic liquid. Larger number of droplet formation was aided by the cosurfactant. Sensitivity towards temperature decreased with increasing amount of cosurfactant, as revealed through the combined dynamic light scattering and viscosity measurements. Oxyethylene group of Tween 20 formed coordinate linkages with the IL cation, which resulted in the rigidity of the polar domain. The IL, in excess of the amount required for coordinating the surfactant head groups, behaved like the bulk component as revealed through the fluorescence anisotropy measurements. Electron microscopy and small angle neutron scattering studies could further shed light on the morphology of the microemulsion droplets, which are considered as the future perspective.